

# Predicting the global mammalian viral sharing network using phylogeography

Gregory F Albery<sup>1,2,3\*</sup>, Evan A Eskew<sup>1</sup>, Noam Ross<sup>1</sup>, Kevin J Olival<sup>1\*</sup>

1. EcoHealth Alliance, New York, NY, USA

2. Institute of Evolutionary Biology, University of Edinburgh, Edinburgh, Scotland

3. Department of Biology, Georgetown University, Washington, DC, USA

\*Corresponding authors: [gfalbery@gmail.com](mailto:gfalbery@gmail.com); [olival@ecohealthalliance.org](mailto:olival@ecohealthalliance.org)

## Abstract

Understanding interspecific viral transmission is key to understanding viral ecology and evolution, disease spillover into humans, and the consequences of global change. Prior work has demonstrated that macroecological factors drive viral sharing in some mammalian groups, but analyses have never attempted to predict viral sharing in a pan-mammalian context. Here we show that host phylogenetic similarity and geographic range overlap are strong, nonlinear predictors of viral sharing among species across the entire mammal class. Using these traits, we predict global viral sharing patterns across 4196 mammal species and show that our simulated network successfully predicts viral sharing and reservoir host status using internal validation and an external dataset. We predict high rates of mammalian viral sharing in the tropics, particularly among rodents and bats, and that within- and between-order sharing differs geographically and taxonomically. Our results emphasize the importance of macroecological factors in shaping mammalian viral communities, and provide a robust, general model to predict viral host range and guide pathogen surveillance and conservation efforts.

27 Most emerging human viruses originate in wild mammals, so understanding the drivers of  
28 interspecific viral transmission in these taxa is an important public health research priority<sup>1,2</sup>.  
29 Despite a rapidly expanding knowledge base, the mammalian viruses known to science  
30 remain taxonomically biased and limited in scope, likely comprising less than 1% of the  
31 complete mammalian virome<sup>3,4</sup>. Furthermore, host range is inadequately characterized even  
32 for the best-studied viruses<sup>5-7</sup>. To help prioritise viral discovery efforts and zoonotic disease  
33 surveillance in wildlife, studies have revealed high (zoonotic) parasite diversity in certain  
34 host taxa, such as rodents and bats<sup>5,8</sup>, and/or linked parasite diversity with host phenotypic  
35 traits such as reproductive output<sup>9,10</sup>. Viral diversity has also been associated with host  
36 macroecological traits, including geographic range size<sup>11</sup> and sympatry with other mammals<sup>5</sup>.  
37 The rationale for investigating viral diversity is that species with more viruses will generate  
38 more opportunities for viral transmission to other species, including humans. However, in  
39 order to infect a new host species, a virus must transmit, invade, and potentially replicate  
40 within the novel host<sup>12</sup>. Each of these processes becomes less likely if the two hosts differ  
41 more in terms of their geographic range, behaviour, and/or biochemistry (i.e., cellular  
42 receptors allowing viral attachment and invasion)<sup>12,13</sup>. Consequently, the probability that a  
43 pair of hosts will share a virus is shaped both by the species' underlying viral diversity and by  
44 species interactions represented by pairwise measures such as spatial overlap, phylogenetic  
45 relatedness, and ecological similarity<sup>14-16</sup>.

46  
47 Previous investigations into pairwise determinants of viral sharing have been limited to one  
48 or two host orders (e.g., bats<sup>17,18</sup>, primates<sup>19</sup>, ungulates<sup>16</sup>, and carnivores<sup>14,16</sup>), while  
49 sometimes lumping together different types of pathogen (e.g., helminths, viruses, and  
50 bacteria). Viruses are sometimes shared across large host phylogenetic distances (e.g., Nipah  
51 virus in bats and pigs, among many others<sup>20,21</sup>), requiring a broader understanding of viral  
52 sharing across mammals to predict patterns at different taxonomic and geographic scales. In  
53 addition, many mammalian orders have yet to be investigated in these analyses – most  
54 notably rodents, which are highly diverse and host important zoonotic viruses<sup>5,8</sup>. In addition,  
55 although phylogenetic and geographic viral sharing effects have been empirically  
56 demonstrated, the models have not yet been applied to validate viral sharing predictions using  
57 external datasets or make inferences about mammals with no known viral associations. If  
58 geographic and phylogenetic effects on viral sharing are as ubiquitous as they seem, these  
59 variables alone could provide a useful baseline model of viral sharing applicable across the  
60 mammal class.

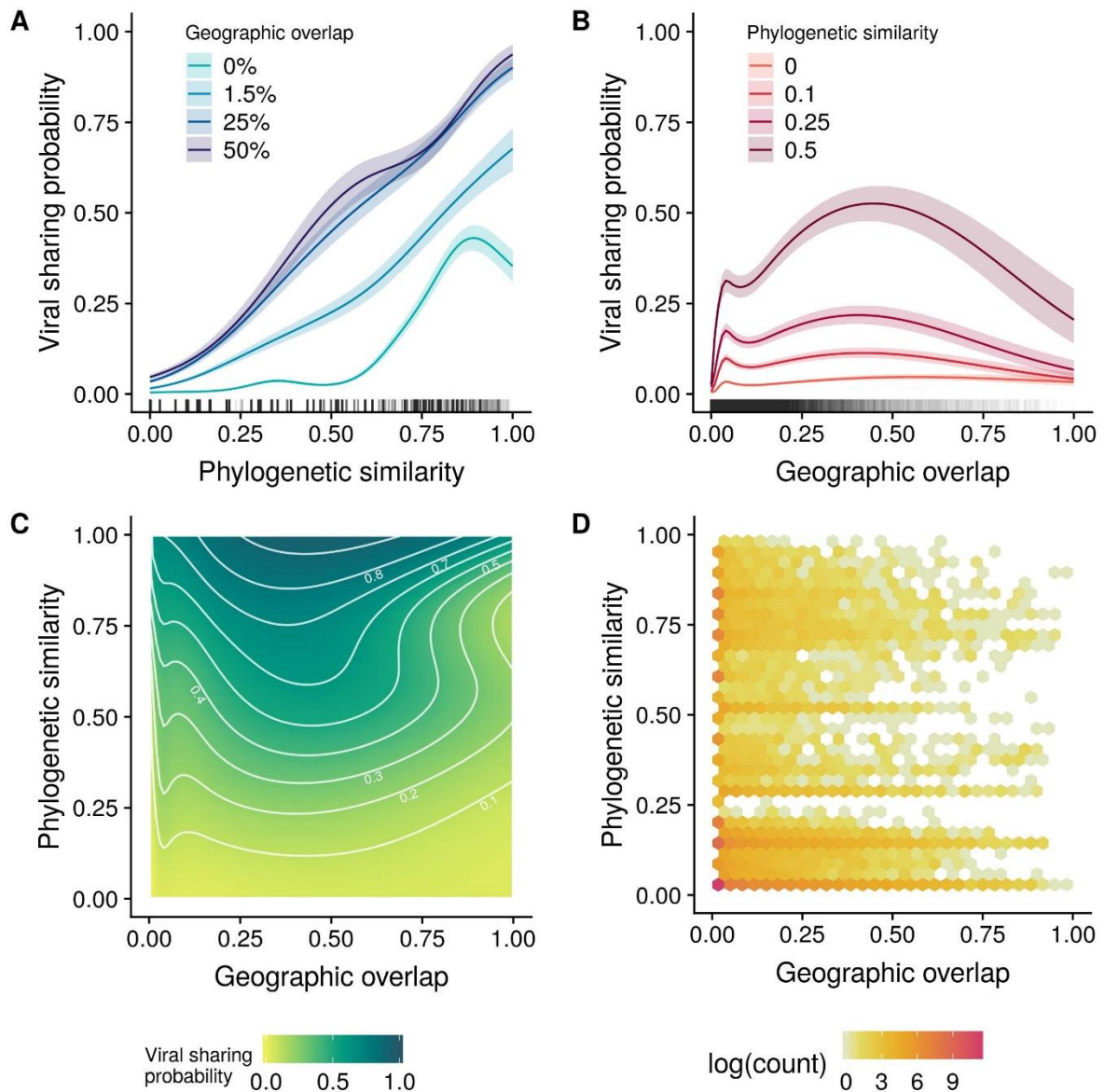
61 Here, we analyse pairwise viral sharing using a novel, conservative modelling approach  
62 designed to partition the contribution of species-level traits from pairwise phylogeographic  
63 traits. This method of analysis stands in contrast to previous studies of mammalian viral  
64 sharing which have mainly focussed on host-level traits, and importantly buffers against  
65 certain inherent biases in the observed viral sharing network, including host sampling bias,  
66 when making predictions.

## 67 **Results and Discussion**

### 68 **Predictors of viral sharing**

69 We fitted a model designed to partition the contribution of species-level effects and pairwise  
70 similarity measures to mammalian viral sharing probability. We used a published database of  
71 1920 mammal-virus associations (excluding humans) as a training dataset<sup>5</sup>. These data  
72 included 591 wild mammal species, equalling 174345 pairwise host species combinations,  
73 with 6.4% connectance – that is, 6.4% of species pairs shared at least one virus. We used a  
74 generalised additive mixed model (GAMM) framework, including a species-level effect in  
75 our model as a multi-membership random effect, capturing variation in each species'  
76 connectedness and underlying viral diversity (see Methods). Overall, our model accounted  
77 for 44.8% of the total deviance in pairwise viral sharing, with 51.1% of this explained  
78 deviance attributable to the identities of the species involved (i.e., the species-level effect).  
79 Our model structure was effective at controlling for species-level variation in our dataset: i.e.,  
80 the term had a strong impact on the centrality of each species when we simulated networks  
81 using just these parameters (Figure SI1). This observation suggests that ~50% of the dyadic  
82 structure of observed viral sharing networks (in contrast to the true underlying network) is  
83 determined by uneven sampling and concentration on specific species, and the remainder by  
84 macroecological processes.

85



86

87 Figure 1: Viral sharing GAMM model outputs and data distribution. A: predicted viral sharing  
88 probability increases with increasing phylogenetic relatedness; the different coloured lines represent  
89 different geographic overlap values. B: predicted viral sharing probability increases with increasing  
90 geographic overlap; the different coloured lines represent different phylogenetic relatedness values. C:  
91 the geographic overlap:phylogenetic similarity interaction surface, where the darker colours represent  
92 increased probability of viral sharing. White contour lines denote 10% increments of sharing  
93 probability. Labels have been removed from some contours to avoid overplotting. D: hexagonal bin  
94 chart displaying the data distribution, which was highly aggregated at low values of phylogenetic  
95 similarity and especially of geographic overlap.

96

97 As expected, increasing host phylogenetic similarity and geographic overlap were associated  
98 with increased probability of viral sharing across mammals, together accounting for the

99 remaining 49% of explained model deviance (Figure 1A-C). Geography, phylogeny, and their  
100 interaction all showed strong nonlinear effects, with geographic overlap in particular driving  
101 a rapid increase in viral sharing that began at ~0-5% range overlap values, peaked at 50%  
102 overlap values, and then levelled off (Figure 1B). This effect closely mirrors previous  
103 observations of strong, nonlinear effects of geographic and phylogenetic similarity  
104 determining within-order viral sharing<sup>14,16-19</sup>. Although occupying little of the visual space  
105 within the model presentation, 93% of mammal pairs had less than 5% spatial overlap (Figure  
106 1B,D). The great majority (86%) of mammal pairs in our dataset did not overlap  
107 geographically and rarely shared viruses unless phylogenetic similarity exceeded ~0.5  
108 (Figure 1A). This phylogenetic distance corresponds roughly to order-level similarity; that is,  
109 if two species did not overlap in space, it was highly unlikely that they shared a virus unless  
110 they were within the same taxonomic order (8% of pairs). Notably, phylogenetic similarity  
111 accounted for more than twice as much model deviance as did spatial overlap (33.8% vs  
112 14.4%). The greater importance of phylogeny relative to geography contrasts with previous  
113 analyses concerning viral sharing in primates<sup>19</sup> and ungulates<sup>16</sup>, likely reflecting the wider  
114 phylogenetic range of hosts considered here. This finding supports the important role of  
115 mammalian evolutionary history in shaping contemporary patterns of viral sharing and  
116 diversity<sup>5,22</sup>.

117

118 In contrast to geography and phylogeny, minimum citation count and domestication status  
119 accounted for a vanishingly small amount of the deviance in viral sharing probability (0.2%  
120 and 0.1%, respectively) even though they have important effects on observed viral diversity  
121 in this dataset<sup>5</sup>. Their impacts on viral sharing may have been largely accounted for by  
122 species-level random effects.

123

124 Our use of a pan-mammalian viral sharing dataset with a large sample size allowed us to  
125 investigate how geographic overlap and phylogenetic similarity affect viral sharing across  
126 different viral subgroups. These subgroups included RNA viruses, vector-borne RNA viruses,  
127 non-vector-borne RNA viruses, and DNA viruses. The importance of geographic overlap  
128 varied widely across all groups of viruses (Figure SI2; Table SI1), while the influence of host  
129 phylogenetic relatedness was more consistent (Figure SI3; Table SI1). Generally, host  
130 phylogeny was more important in determining sharing of DNA viruses than it was for RNA  
131 viruses, while space sharing was more important for vector-borne RNA viruses, and less so  
132 for non-vector-borne RNA viruses. These results likely reflect important aspects of viral

133 ecology, transmission, and evolution: for example, RNA viruses are fast-evolving, allowing  
134 them to more quickly adapt to novel hosts, such that phylogenetic distances are less important  
135 in determining viral sharing patterns<sup>23</sup>. Conversely, DNA viruses are more evolutionarily  
136 constrained, with an evolutionary rate typically <1% that of RNA viruses, such that  
137 phylogenetic distance between hosts presents a more significant obstacle for sharing of DNA  
138 viruses<sup>24</sup>. The profound importance of geographic overlap in shaping the viral sharing  
139 network for vector-borne RNA viruses (Figure SI3) likely emerges from the geographic  
140 distributions and ecological constraints placed on vectors, lending further support to efforts to  
141 model the global spread of arboviruses by predicting changes in their vectors' distributions  
142 and ecological niches<sup>25,26</sup>. Generally, the fact that viral sharing across different viral  
143 subgroups was predicted by different macroecological relationships suggests they should be  
144 examined separately in future analyses where possible.

## 145 **Predicting pan-mammalian viral sharing**

146 Previous trait-based approaches to predict viral sharing and reservoir hosts have been  
147 hindered by incomplete and inconsistent characterization of traits central to those modelling  
148 efforts. In contrast, spatial distributions and phylogenetic data are readily available and  
149 uniformly quantified for the vast majority of mammals and, as we have shown, are reliable  
150 predictors of viral sharing (>20% of total deviance). Thus, we used our GAMM estimates to  
151 predict unobserved global viral sharing patterns across 8.8 million mammal-mammal pairs  
152 using a database of geographic distributions<sup>27</sup> and a recent mammalian supertree<sup>28</sup> (see  
153 Methods). The predicted network included 4196 (non-human) Eutherian mammals with  
154 available data, 591 of which were recorded with viral associations in our training data. We  
155 calculated each species' predicted degree centrality, as a simple and interpretable network-  
156 derived measure of viral sharing: that is, the number of other mammal species a given  
157 mammal species is expected to share at least one virus with. We identified geographic and  
158 taxonomic trends in degree centrality, validated our predicted sharing network using an  
159 external dataset, and simulated reservoir identification to assess host predictability for focal  
160 viruses (see Methods).

161

162 We confirmed that our modelled network recapitulated expected patterns of viral sharing  
163 using the Enhanced Infectious Diseases Database (EID2) as an external dataset<sup>29</sup>. This dataset  
164 was constructed by mining web-based sequence data to identify host-pathogen associations,

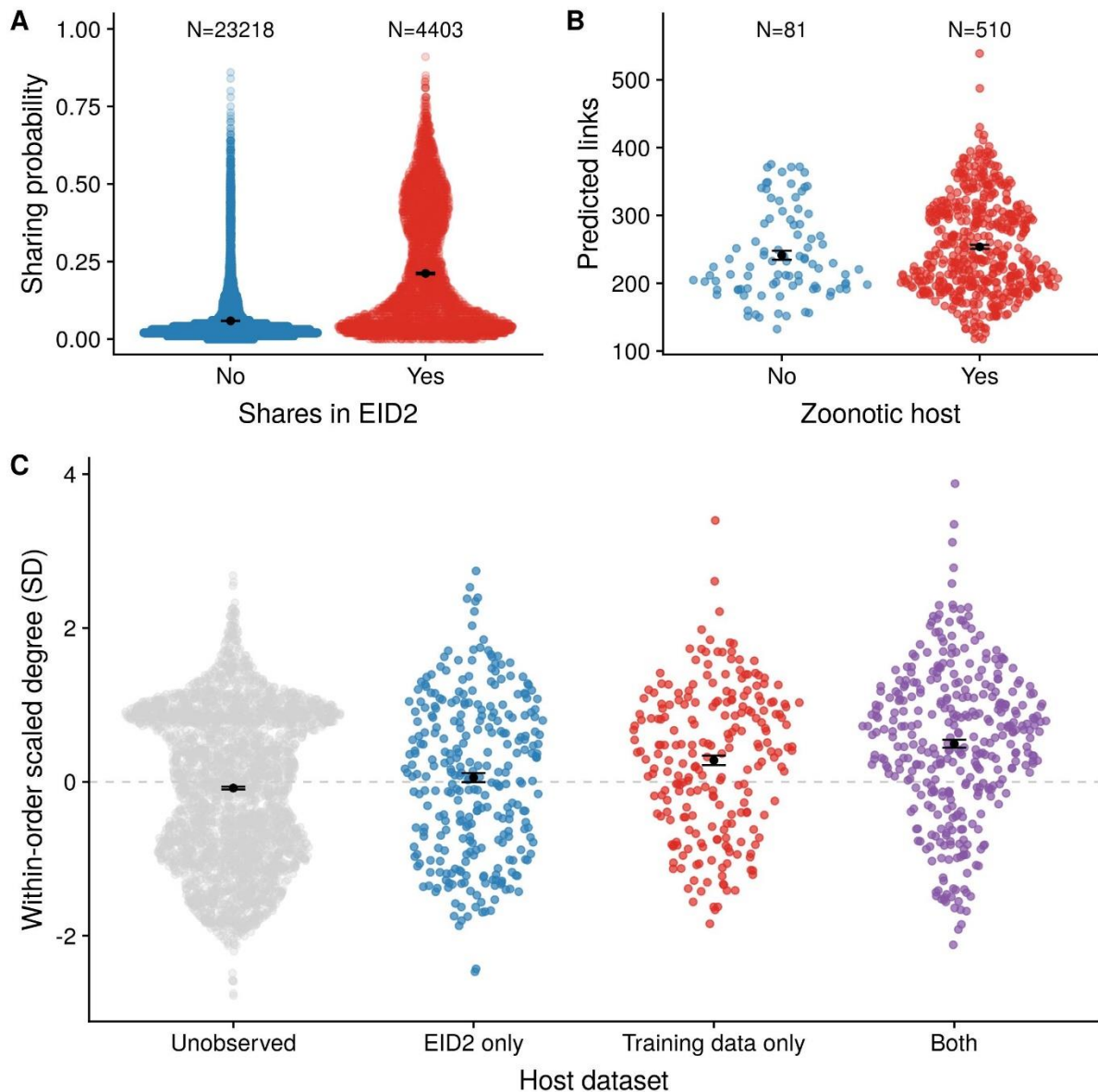
165 many of which are mammal-virus interactions<sup>29</sup>. Pairs of species that share viruses in EID2,  
166 but which were not in our training dataset (see Methods), had a much higher mean sharing  
167 probability in our predicted network (20% versus 5%; Figure 2A). In addition, more central  
168 species in the predicted network were more likely to have been observed with a virus,  
169 whether zoonotic (Figure 2B) or non-zoonotic (Figure 2C), implying that the predicted  
170 network accurately captured realised potential for viral sharing and zoonotic spillover. This  
171 finding concurs with similar work in primates which demonstrated that high centrality in  
172 primate-parasite networks is associated with carriage of zoonoses<sup>30</sup>. We corroborate these  
173 findings considering all mammal-mammal viral sharing links, not just zoonotic links, and  
174 show that for each mammalian order, species with higher degree centrality in our predicted  
175 network are more likely to have been observed with viruses in the EID2 dataset (Figure 2C;  
176 Figure SI4). It is possible that species with higher centrality in the global viral sharing  
177 network are more important for viral sharing, and thus have been more likely to be observed  
178 with a (zoonotic) virus. Species that are more central in our predicted network could therefore  
179 be prioritised for zoonotic surveillance or sampling in the event of viral outbreaks with  
180 unknown mammalian origins. Given that mammal diversity predicts patterns of livestock  
181 disease<sup>31</sup> and zoonoses<sup>32</sup>, the geographic patterns of degree centrality predicted here (Figure  
182 3, Figure SI5; see below) could also be used as a coarse predictor of viral disease risk to  
183 livestock and human health, providing additional insights that emerge from the joint,  
184 nonlinear effects of geography and phylogeny as opposed to examination of their effects in  
185 isolation. Similarly, where there is limited knowledge of mammalian host range for newly-  
186 discovered viruses, our modelled network can be used to prioritise the sampling of additional  
187 species for viral surveillance.

188

189 The high predicted centrality of known hosts may be due partly to selective sampling (i.e.,  
190 viral researchers are more likely to sample wide-ranging and common host species that also  
191 share viruses with many other species<sup>10,20</sup>). This possibility is supported by the increased  
192 degree centrality for species that appear in both EID2 and our dataset rather than in only one  
193 of the two, as these species are presumably more well-known (Figure 2C). Similarly, while  
194 we believe that our model was successful at accounting for variation in host-level diversity  
195 and study effort that influences network topology (see above; Figure SI1), there are certain  
196 inherent biases in the training data which must be considered when interpreting our findings.  
197 Most notably, viral sharing estimates in our dataset may be affected by the fact that zoonotic  
198 discovery efforts commonly search limited geographic regions for a specific virus or group of

199 viruses, artificially increasing the likelihood of detecting these viruses in the same region  
200 compared to a geographically random sampling regime. Moreover, when a mammal species  
201 (e.g., a bat) is found with a focal virus (e.g., an ebolavirus), it is logical for researchers to then  
202 investigate similar, closely related species in nearby locales<sup>33</sup>. These sampling approaches  
203 could disproportionately weight the network towards finding phylogeographic effects on viral  
204 sharing probability. However, it is highly encouraging that our model predicted patterns in  
205 the external EID2 dataset, which was constructed using different data compilation methods  
206 but also comprises global data covering several decades of research<sup>29</sup>. In sum, we believe that  
207 our approach is a conservative method for minimising the biases inherent in the data. The  
208 knowledge that the observed mammalian virome is biased ultimately calls for more uniform  
209 viral sampling across the mammal class and increased coverage of rarely-sampled groups,  
210 lending support to ongoing efforts to systematically catalogue mammalian viral diversity<sup>3</sup>.





211  
212

213 Figure 2: The modelled mammalian viral sharing network predicts observed viral sharing trends in an  
214 independent dataset. In all figures, points are jittered along the x axis according to a density function;  
215 the black points and associated error bars are means  $\pm$  standard errors. A: species pairs with higher  
216 predicted viral sharing probability from our model were more likely to be observed sharing a virus in  
217 the independent EID2 dataset. This comparison excludes species pairs that were also present in our  
218 training data. B: species that hosted a zoonotic virus in our dataset had more viral sharing links in the  
219 predicted all-mammal network than those without zoonotic viruses. C: species that had never been  
220 observed with a virus have fewer links in the predicted network than species that hosted viruses in the  
221 EID2 dataset only, in our training data only, or in both. The y axis represents viral sharing link  
222 number, scaled to have a mean of 0 and a standard deviation of 1 within each order for clarity. Figure  
223 SI4 displays these same data without the within-order scaling.

## 224 **Taxonomic and geographic patterns of predicted viral** 225 **sharing**

226 Our network predicted strong taxonomic patterns in the probability of viral sharing. Looking  
227 across mammalian orders, rodents (Rodentia) and bats (Chiroptera) had the most predicted  
228 species-level viral links, while carnivores and artiodactyl ungulates had substantially fewer  
229 (Figure 3A). Examining multiple mammalian orders allowed us to partition the predicted  
230 sharing network into within- and between-order links to investigate whether certain orders are  
231 better-connected to other orders. Indeed, this partitioning revealed differences in taxonomic  
232 and geographic patterns of viral sharing. In bats and rodents, large numbers of within-order  
233 links are driven by high within-order species diversity (Figure 3C). Interestingly, when  
234 within-order links were ignored, leaving only out-of-order links, rodents and bats were  
235 among the least-connected Eutherian orders (Figure 3E), while even-toed ungulates and  
236 carnivores were ranked among the most-connected (Figure 3E). Taken together, these results  
237 imply that while bats and rodents are important in viral sharing networks, their sharing is  
238 mainly restricted to other bats and rodents, respectively. This distinction only applied to mean  
239 link numbers; when link numbers were summed, rodents and bats remained highly connected  
240 regardless of which metric was used, as a result of their species richness (Figure SI5).

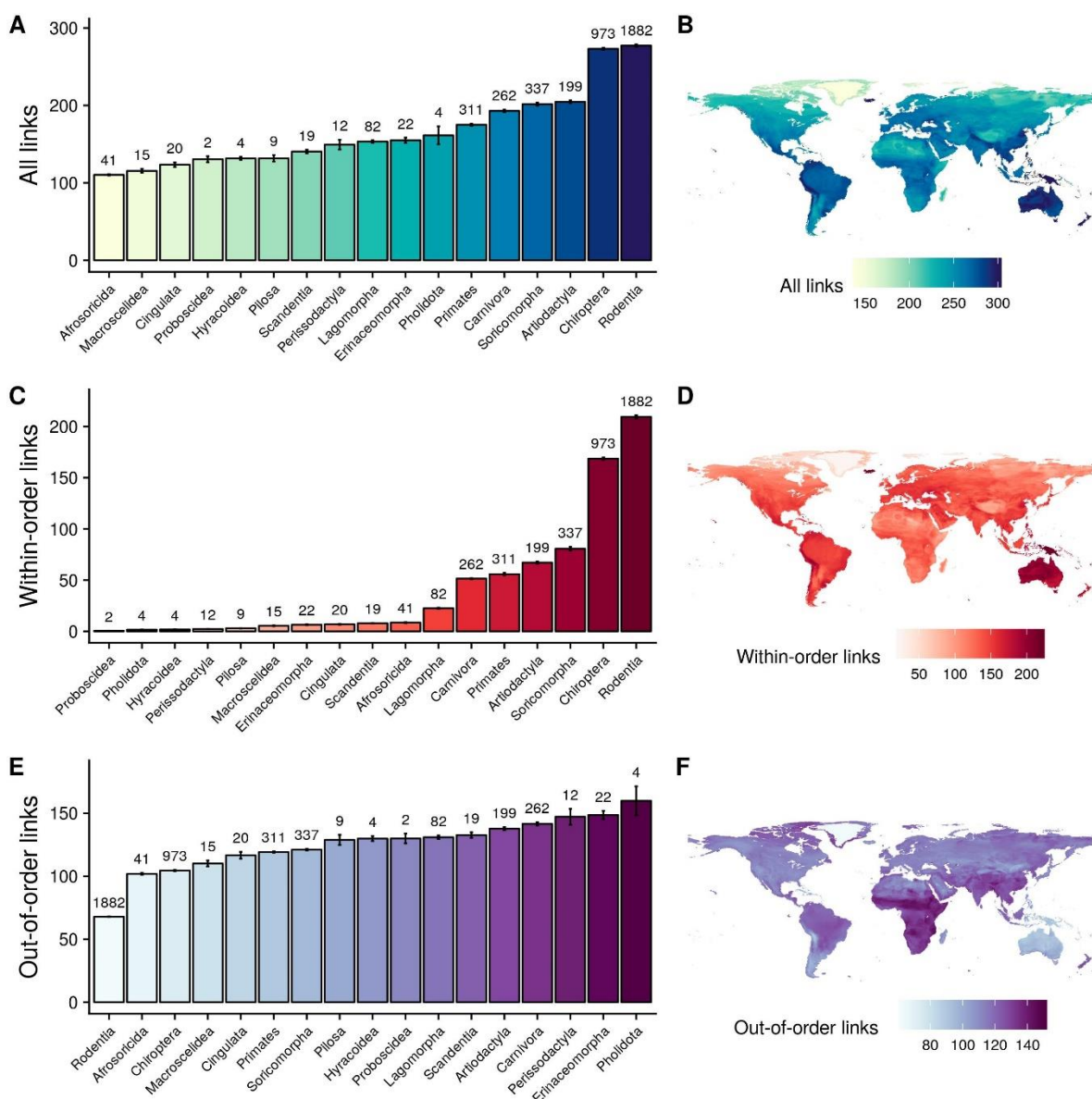
241  
242 Previous analyses have demonstrated that both bats and rodents are important for hosting  
243 zoonotic viruses, with possible explanations including species-level phenotypic traits such as  
244 behaviour<sup>5</sup>, life history<sup>9</sup>, or metabolic idiosyncracies<sup>34</sup>. Our results imply that while both  
245 orders potentially host many zoonoses purely as a result of their species richness (Figure  
246 SI5), the vast majority of their viral sharing occurs within-order even though larger  
247 phylogenetic jumps are necessary for spillover. Intriguingly, recent work has shown that  
248 infection of an aggregated phylogenetic selection of hosts is an important contributor to viral  
249 zoonotic potential<sup>35</sup>. Rodents' and bats' tendency towards high viral interconnectedness could  
250 encourage viruses to achieve such aggregation, leading to opportunities for spillover into  
251 humans. In our analysis, both orders' high centrality emerged purely as a result of their  
252 phylogenetic diversity and geographic distributions, rather than from other phenotypic traits.  
253 If well-connected species in our network are more likely to maintain a high diversity of  
254 viruses (e.g., via multi-host dynamics leading to an expanded threshold population size<sup>36</sup>),  
255 this may contribute to the high viral diversity documented in bats and rodents<sup>5</sup>. Efforts to  
256 prioritise viral sampling regimes should consider biogeography and mammal-mammal

257 interactions in addition to searching for species-level traits associated with high viral  
 258 diversity.

259

260 Encouragingly, our network showed predictable scaling laws similar to those of other known  
 261 ecological networks<sup>37</sup>. Viral link numbers in within-order subnetworks (e.g., between  
 262 different bat species) correlated strongly with species diversity within each order ( $R^2 \sim 0.85$ ),  
 263 following a power law with a Z value of  $\sim 0.8$  (Figure SI6). Similarly, out-of-order links (e.g.,  
 264 between a bat and a rodent) scaled linearly with the product of the species richness of both  
 265 orders (Figure SI7).

266



267

268 Figure 3: Taxonomic and geographic patterns of mean predicted viral sharing link numbers (degree centrality).

269 Top row: all viral sharing links; middle row: viral sharing links with species in the same order; bottom row:

270 viral sharing links with species in another order. A,C,E: average species-level viral sharing link numbers for  
271 mammalian orders in our dataset. Bars represent means; error bars represent standard errors. B,D,F: geographic  
272 distributions of mean viral sharing link numbers. Distributions were derived by summing the viral sharing link  
273 numbers of all species inhabiting a 25km<sup>2</sup> grid square and dividing them by the number of species inhabiting the  
274 grid square, giving mean degree number at the grid level.

275

276 To visualize geographic patterns of viral sharing, we projected species-level degree centrality  
277 across the species' ranges then calculated grid cell-level mean degree centrality (Figure 3B),  
278 as well as summed degree centrality (Figure SI5). Average centrality peaked in tropical areas  
279 of South and Central America, Sub-Saharan Africa, and Southeast Asia, especially in the  
280 Andes and Himalayas (Figure 3B). These patterns align with previously-reported hotspots of  
281 emerging zoonoses and predicted viral diversity<sup>5,32</sup> and imply that areas of high biodiversity  
282 are centres of viral sharing not just because of the number of overlapping species (i.e., high  
283 species richness), but also because more closely related species create a more connected viral  
284 sharing network in these areas. This densely-connected network structure and the increased  
285 biomass present in the tropics might have synergistic implications for cross-species  
286 maintenance and transmission of viral diversity in these areas. The geographic distributions  
287 of mean predicted within- and between-order viral links differed notably from the distribution  
288 of interspecific links generally: the relative importance of South America and East Asia was  
289 higher for within-order links (Figure 3D), while Sub-Saharan Africa remained a hotspot for  
290 out-of-order links (Figure 3F). Geographic patterns of summed link numbers more closely  
291 mirrored underlying host species richness, whether for all links, within-order links, or out-of-  
292 order links (Figure SI5).

293

294 We acknowledge that our phylogeographic model of viral sharing does not account for  
295 complex ecological interactions such as coinfection or coevolution, which could impact how  
296 patterns of exposure and host susceptibility translate to realised viral diversity. Future  
297 investigations could extend our framework to simulate the dynamic co-speciation of  
298 mammals and their viruses in order to account for these processes and/or to explicitly  
299 investigate how viral sharing connectivity and viral diversity are correlated across mammal  
300 species. Our model may also prove useful for building and parameterising much-needed  
301 multi-host network models for conservation purposes, particularly where there is scarce prior  
302 information on interspecific pathogen sharing<sup>36,38</sup>.

303

## 304 **The network as a predictive tool**

305 Identifying potential hosts for known and novel viruses is an important component of  
306 preemptive zoonotic disease surveillance that can speed public health responses. Predictive  
307 techniques based on species-level phenotypic and genomic data have been suggested to help  
308 prioritise sampling targets<sup>6,7,9</sup>. Although these approaches represent a promising  
309 methodological advance, they may not elucidate the mechanistic underpinnings of viral host  
310 range, reducing their potential efficacy for guiding public health interventions. In addition,  
311 genomic approaches require viral sequence data, which can be time-consuming and  
312 operationally challenging to acquire or share publicly. We therefore interrogated our  
313 predicted viral sharing network to investigate whether it could be used to identify potential  
314 hosts of known viruses at the species level. Using a leave-one-out prediction process (see  
315 Methods), our model showed a surprisingly strong ability to predict observed host species for  
316 250 viruses with at least two known (non-human) mammal hosts.

317  
318 We investigated the predictive potential of our model by iteratively selecting all but one of  
319 the known hosts for a given virus, then using the predicted sharing patterns of the remaining  
320 hosts to identify how the focal (removed) host was ranked in terms of its sharing probability.  
321 In practical terms, these species-level rankings could set sampling priorities for public health  
322 efforts seeking to identify hosts of a novel zoonotic virus, where one or more hosts are  
323 already known. Across all 250 viruses, the median ranking of the left-out host was 72 out of a  
324 potential 4196 mammals (i.e., in the top 1.7% of potential hosts). To compare this ranking to  
325 alternative heuristics, we examined how high the focal host would be ranked using simple  
326 ranked phylogenetic relatedness or spatial overlap values alone (i.e., the most closely-related,  
327 followed by the second-most-related, etc.). Using this method, the focal host was ranked  
328 288th (for phylogeny) or 283rd (for space), identifying the focal host in the top 7% of  
329 potential hosts and demonstrating that sampling prioritization schemes based on our  
330 phylogeographic model would require only  $\frac{1}{4}$  as many sampling targets in order to identify  
331 the correct sharing host. Our model therefore represents a substantial improvement over  
332 search methods that involve only spatial or phylogenetic similarity. Our model performed  
333 similarly at identifying focal hosts in the EID2 dataset<sup>29</sup>: for the 109 viruses in the EID2  
334 dataset with more than one host, the focal host was identified in the top 63 (1.5%) potential  
335 hosts. In contrast, ranked spatial overlap predicted the focal host in the top 560 hosts, and  
336 phylogenetic relatedness in the top 174.

337

338 We observed substantial variation in our model's ability to predict known hosts among  
339 different viruses. For example, the correct host was predicted first in every iteration for 7  
340 viruses and in the top 10 hosts for 42 viruses. Results for 128 viruses had the focal host  
341 falling within the top 100 guesses, and for only 6 viruses were the model-based host searches  
342 worse than chance (focal host ranked lower than 50% of all mammals in terms of sharing  
343 probability). We used this measure of viral sharing “predictability” to investigate whether  
344 certain viral traits affected the ease with which phylogeography predicted their hosts. Viruses  
345 with broad host phylogenetic ranges, most notably Ebola virus, challenge reservoir prediction  
346 efforts since many more species must often be sampled before identifying the correct host(s).  
347 To investigate whether the predictive strength of our model was limited for viruses with  
348 broad host ranges and/or other viral traits, we fitted a linear mixed model (LMM) which  
349 showed a strong negative association between viruses’ known phylogenetic host breadth and  
350 the predictability of focal hosts (model  $R^2=0.70$ ; host breadth  $R^2=0.67$ ; Figure SI9). This  
351 association demonstrates, unsurprisingly, that predicting the hosts of generalist viruses is  
352 intrinsically difficult using our method. This adds a potential limitation to the applicability of  
353 our network approach, given that zoonotic viruses commonly exhibit wide host ranges<sup>2,5</sup>. A  
354 family-level random effect accounted for little of the apparent variance in predictability  
355 among viral families (Figure SI8).

356

357 Once viral host range was accounted for, hosts of vector-borne viruses were slightly easier to  
358 predict than non-vector-borne viruses ( $R^2=0.1$ ; Figure SI9) – perhaps because the sharing of  
359 vector-borne viruses depends more heavily on host geographic distributions (Figure SI3).  
360 Despite additional variation in the data, no other viral traits (e.g., RNA vs. DNA, segmented  
361 vs. non-segmented) were important in the LMM. This implies that host phylogeographic  
362 traits are a good broad-scale indicator of viral sharing, particularly when ecological specifics  
363 of the virus itself are unknown.

364

## 365 **Conclusion**

366 In summary, we present a simple, highly interpretable model that predicted a substantial  
367 proportion of viral sharing across mammals and is capable of identifying species-level  
368 sampling priorities for viral surveillance and discovery. It is worth noting that the analytical

369 framework and validation we describe were conducted on a global scale, while many  
370 zoonotic sampling efforts occur on a national or regional scale. Restricting the focal  
371 mammals to a regional pool may improve the applicability of our model in certain sampling  
372 contexts, and future studies could leverage higher-resolution phylogenetic and geographic  
373 data to fine-tune predictions. In particular, the mammalian supertree<sup>28</sup> has relatively poor  
374 resolution at the species tips such that relatedness estimates based on alternative molecular  
375 evidence (e.g., full host genome data) may allow more precise estimates of the phylogenetic  
376 relatedness effect on viral sharing. Alternatively, our model could be augmented with  
377 additional host, virus, and pairwise traits, using similar pairwise formulations of viral sharing  
378 as a response variable, to identify ecological specificities that are critical for the transmission  
379 of certain viruses, to partition viral subtypes, and, ultimately, to increase the accuracy of host  
380 prediction. By generalising the spatial and phylogenetic processes that drive viral sharing, our  
381 model serves as a useful guide for the prioritization of viral sampling, presenting a baseline  
382 for future modelling efforts to compare against and improve upon.

383

384 Our ability to model and predict macroecological patterns of viral sharing is important in an  
385 era of rapid global change. Under all conceivable global change scenarios, many mammals  
386 will shift their geographic ranges, whether of their own volition or through human assistance.  
387 Mammalian parasite communities will likely undergo considerable rearrangement as a result,  
388 with potentially far-reaching ecological consequences<sup>39-41</sup>. Our findings suggest that novel  
389 species encounters will provide opportunities for interspecific viral transmission, which could  
390 be facilitated by even relatively small changes in range overlap. These future cross-species  
391 transmission events will have profound implications for conservation and public health,  
392 potentially devastating populations of host species without evolved resistance to the novel  
393 viruses (e.g., red squirrel declines brought about by parapoxvirus infections spread by  
394 introduced grey squirrels<sup>42</sup>) or increasing zoonotic disease risk by introducing viruses to  
395 human-adjacent amplifier hosts (e.g., horses increasing the risk of human infection with  
396 Hendra virus<sup>20</sup>). Thus, our global model of mammalian viral sharing provides a crucial  
397 complement to ongoing work modelling the spread of hosts, vectors, and their associated  
398 diseases as the result of climate change-induced range expansions<sup>25,39</sup>.

## 399 **Acknowledgements**

400 This work was conducted during a placement funded by the National Environmental  
401 Research Council (NERC) Overseas Research Fund awarded to GFA. GFA's PhD  
402 studentship was likewise funded by NERC (grant number: NE/L002558/1). EAE, NR, and  
403 KJO were funded by the generous support of the American people through the United States  
404 Agency for International Development (USAID) Emerging Pandemic Threats PREDICT  
405 project. Additional support was provided by the National Institute of Allergy and Infectious  
406 Diseases of the National Institutes of Health (Award Number R01AI110964) and the US  
407 Department of Defense, Defense Threat Reduction Agency (HDTRA11710064). We thank  
408 Colin Carlson, Verity Hill, and members of EcoHealth Alliance for advice and helpful  
409 comments on the manuscript.

## 410 **Author contributions**

411 GFA, EAE, NR, and KJO designed the study together. GFA conducted the analyses under  
412 NR's supervision. GFA wrote the manuscript, while EAE, NR, and KJO offered comments  
413 and edits to the manuscript throughout.

## 414 **References**

- 415 1. Woolhouse, M. E. J. & Gowtage-Sequeria, S. Host range and emerging and reemerging  
416 pathogens. *Emerg. Infect. Dis.* **11**, 1842–7 (2005).
- 417 2. Johnson, C. K. *et al.* Spillover and pandemic properties of zoonotic viruses with high host  
418 plasticity. *Sci. Rep.* **5**, 1–8 (2015).
- 419 3. Carroll, D. *et al.* The Global Virome Project. *Science (80-. )*. **359**, 872–874 (2018).
- 420 4. Carlson, C. J., Zipfel, C. M., Garnier, R. & Bansal, S. Global estimates of mammalian viral  
421 diversity accounting for host sharing. *Nat. Ecol. Evol.* **3**, 1070–1075 (2019).
- 422 5. Olival, K. J. *et al.* Host and viral traits predict zoonotic spillover from mammals. *Nature* **546**,  
423 646–650 (2017).
- 424 6. Han, B. A. *et al.* Undiscovered Bat Hosts of Filoviruses. *PLoS Negl. Trop. Dis.* **10**, e0004815  
425 (2016).
- 426 7. Babayan, S. A., Orton, R. J. & Streicker, D. G. Predicting reservoir hosts and arthropod  
427 vectors from evolutionary signatures in RNA virus genomes. *Science (80-. )*. **362**, 577–580  
428 (2018).
- 429 8. Luis, A. D. *et al.* A comparison of bats and rodents as reservoirs of zoonotic viruses: are bats  
430 special? *Proc. R. Soc. B Biol. Sci.* **280**, 20122753 (2013).
- 431 9. Han, B. A., Schmidt, J. P., Bowden, S. E. & Drake, J. M. Rodent reservoirs of future zoonotic  
432 diseases. *Proc. Natl. Acad. Sci.* **112**, 7039–7044 (2015).
- 433 10. Plourde, B. T. *et al.* Are disease reservoirs special? Taxonomic and life history characteristics.



- 434 *PLoS One* **12**, e0180716 (2017).
- 435 11. Dallas, T. A. *et al.* Host traits associated with species roles in parasite sharing networks. *Oikos*  
436 **128**, 23–32 (2019).
- 437 12. Plowright, R. K. *et al.* Pathways to zoonotic spillover. *Nat. Rev. Microbiol.* **15**, 502–510  
438 (2017).
- 439 13. Ge, X. Y. *et al.* Isolation and characterization of a bat SARS-like coronavirus that uses the  
440 ACE2 receptor. *Nature* **503**, 535–538 (2013).
- 441 14. Huang, S., Bininda-Emonds, O. R. P., Stephens, P. R., Gittleman, J. L. & Altizer, S.  
442 Phylogenetically related and ecologically similar carnivores harbour similar parasite  
443 assemblages. *J. Anim. Ecol.* **83**, 671–680 (2014).
- 444 15. Wells, K. *et al.* Global spread of helminth parasites at the human-domestic animal-wildlife  
445 interface. *Glob. Chang. Biol.* **24**, 3254–3265 (2018).
- 446 16. Stephens, P. R. *et al.* Parasite sharing in wild ungulates and their predators: Effects of  
447 phylogeny, range overlap, and trophic links. *J. Anim. Ecol.* **88**, 1017–1028 (2019).
- 448 17. Streicker, D. G. *et al.* Host Phylogeny Constrains Cross-Species Emergence and Establishment  
449 of Rabies Virus in Bats. *Science (80-. )*. **329**, 676–679 (2010).
- 450 18. Willoughby, A. R., Phelps, K. L., Predict Consortium, predict@ucdavis.edu & Olival, K. J. A  
451 comparative analysis of viral richness and viral sharing in cave-roosting bats. *Diversity* **9**, 1–16  
452 (2017).
- 453 19. Davies, T. J. & Pedersen, A. B. Phylogeny and geography predict pathogen community  
454 similarity in wild primates and humans. *Proc. R. Soc. B Biol. Sci.* **275**, 1695–1701 (2008).
- 455 20. Glennon, E. E. *et al.* Domesticated animals as hosts of henipaviruses and filoviruses: A  
456 systematic review. *Vet. J.* **233**, 25–34 (2018).
- 457 21. Chua, K. B. *et al.* Nipah Virus: A Recently Emergent Deadly Paramyxovirus. *Science (80-. )*.  
458 **288**, 1432–1435 (2000).
- 459 22. Guy, C., Thiagavel, J., Mideo, N. & Ratcliffe, J. M. Phylogeny matters: Revisiting ‘a  
460 comparison of bats and rodents as reservoirs of zoonotic viruses’. *R. Soc. Open Sci.* **6**, 181182  
461 (2019).
- 462 23. Pybus, O. G., Tatem, A. J. & Lemey, P. Virus evolution and transmission in an ever more  
463 connected world. *Proc. R. Soc. B Biol. Sci.* **282**, 20142878 (2015).
- 464 24. Sanjuán, R., Nebot, M. R., Chirico, N., Mansky, L. M. & Belshaw, R. Viral mutation rates. *J.*  
465 *Virology* **84**, 9733–9748 (2010).
- 466 25. Ryan, S. J., Carlson, C. J., Mordecai, E. A. & Johnson, L. R. Global expansion and  
467 redistribution of Aedes-borne virus transmission risk with climate change. *PLoS Negl. Trop.*  
468 *Dis.* **13**, e0007213 (2019).
- 469 26. Drake, J. M. & Beier, J. C. Ecological niche and potential distribution of *Anopheles arabiensis*  
470 in Africa in 2050. *Malar. J.* **13**, 213 (2014).
- 471 27. IUCN. The IUCN Red List of Threatened Species. *IUCN Red List of Threatened Species.*  
472 *Version 2019-2* (2019). Available at: <https://www.iucnredlist.org>.
- 473 28. Fritz, S. A., Bininda-Emonds, O. R. P. & Purvis, A. Geographical variation in predictors of  
474 mammalian extinction risk: big is bad, but only in the tropics. *Ecol. Lett.* **12**, 538–549 (2009).
- 475 29. Wardeh, M., Risley, C., McIntyre, M. K., Setzkorn, C. & Baylis, M. Database of host-  
476 pathogen and related species interactions, and their global distribution. *Sci. Data* **2**, 150049

- 477 (2015).
- 478 30. Gómez, J. M., Nunn, C. L. & Verdú, M. Centrality in primate-parasite networks reveals the  
479 potential for the transmission of emerging infectious diseases to humans. *Proc. Natl. Acad. Sci.*  
480 **110**, 7738–41 (2013).
- 481 31. Wang, Y. X. G. G. *et al.* Phylogenetic structure of wildlife assemblages shapes patterns of  
482 infectious livestock diseases in Africa. *Funct. Ecol.* **33**, 1332–1341 (2019).
- 483 32. Allen, T. *et al.* Global hotspots and correlates of emerging zoonotic diseases. *Nat. Commun.* **8**,  
484 1124 (2017).
- 485 33. Becker, D. J., Crowley, D. E., Washburne, A. D. & Plowright, R. K. Temporal and spatial  
486 limitations in global surveillance for bat filoviruses and henipaviruses. *Biol. Lett.* **15**,  
487 20190423 (2019).
- 488 34. Xie, J. *et al.* Dampened STING-Dependent Interferon Activation in Bats. *Cell Host Microbe*  
489 **23**, 297–301 (2018).
- 490 35. Park, A. W. Phylogenetic aggregation increases zoonotic potential of mammalian viruses. *Biol.*  
491 *Lett.* **15**, 20190668 (2019).
- 492 36. Lloyd-smith, J. O. *et al.* Epidemic Dynamics at the Human-Animal Interface. *Science (80-. )*.  
493 **326**, 1362–1368 (2009).
- 494 37. Brose, U., Ostling, A., Harrison, K. & Martinez, N. D. Unified spatial scaling of species and  
495 their trophic interactions. *Nature* **108**, 167–171 (2003).
- 496 38. Silk, M. *et al.* Integrating social behaviour, demography and disease dynamics in network  
497 models: applications to disease management in declining wildlife populations. *Philos. Trans.*  
498 *R. Soc. B* **374**, 20180211 (2019).
- 499 39. Carlson, C. J. *et al.* Parasite biodiversity faces extinction and redistribution in a changing  
500 climate. *Sci. Adv.* **3**, e1602422 (2017).
- 501 40. Williams, J. E. & Blois, J. L. Range shifts in response to past and future climate change: Can  
502 climate velocities and species' dispersal capabilities explain variation in mammalian range  
503 shifts? *J. Biogeogr.* **45**, 2175–2189 (2018).
- 504 41. Chen, I.-C., Hill, J. K., Ohlemüller, R., Roy, D. B. & Thomas, C. D. Rapid range shifts of  
505 species associated with high levels of climate warming. *Science (80-. )*. **333**, 1024–6 (2011).
- 506 42. Tompkins, D. M., Sainsbury, A. W., Nettleton, P., Buxton, D. & Gurnell, J. Parapoxvirus  
507 causes a deleterious disease in red squirrels associated with UK population declines. *Proc. R.*  
508 *Soc. B Biol. Sci.* **269**, 529–533 (2002).
- 509 43. R Core Team. R: A language and environment for statistical computing. R Foundation for  
510 Statistical Computing, Vienna, Austria. (2018).
- 511 44. Wood, S. N. Fast stable restricted maximum likelihood and marginal likelihood estimation of  
512 semiparametric generalized linear models. *J. R. Stat. Soc. Ser. B (Statistical Methodol.* **73**, 3–  
513 36 (2011).

514

## 515 **Methods**

### 516 **Making the training data network**

517 Code and data for all analyses are available at  
518 <https://github.com/gfalbery/ViralSharingPhylogeography>. Our dataset included 1920 mammal-  
519 virus associations obtained from an exhaustive literature search which has been used to  
520 investigate how species traits influence mammalian viral diversity<sup>5</sup>. We removed humans and  
521 rabies virus from the dataset as both were disproportionately well-connected, and we  
522 removed 20 non-Eutherian mammals because they were extreme phylogenetic outliers,  
523 leaving 591 Eutherian mammals that shared 401 viruses. We made an unweighted bipartite  
524 network using the mammal-virus associations and projected the unipartite mammal-mammal  
525 network, which we then converted into a sequence of all unique mammal-mammal pairs  
526 where 1/0 denoted whether the pair of species shared a virus or not. This comprised only the  
527 lower triangle of the adjacency matrix to avoid duplicating associations and to remove self-  
528 connections, and only included mammals with at least one sharing link (final N=174345  
529 unique mammal-mammal pairs). 6.4% of these pairs shared at least one virus.

530

531 All analyses were performed in R version 3.6.0<sup>43</sup>. Phylogenetic similarity was calculated  
532 using a mammalian supertree<sup>28</sup> as previously described<sup>5</sup>. Pairwise phylogenetic distances  
533 were defined as the cumulative branch length between the two species and were scaled to  
534 between 0 and 1, and subtracted from 1 to give a measure of relative phylogenetic similarity  
535 (rather than distance). Of the 4716 Eutherian species in the mammalian supertree, 591 had  
536 virus association records in our fully-connected network and 4196 had known geographic  
537 ranges. We used IUCN species ranges to quantify species' geographic distributions<sup>27</sup>. These  
538 range maps are generated based on expert knowledge and only comprise species  
539 presence/absence information rather than density. We converted all range polygons to 25 km<sup>2</sup>  
540 raster grids. For each species-pair, we quantified range overlap as the number of raster grid  
541 squares jointly inhabited by the two species (in the Mollweide projection, which exhibits  
542 equal grid size), divided by the total number of grid squares occupied by these species  
543 combined, so that each value was scaled from 0-1:  $overlap_{A,B} = \text{grid}_{A,B} / (\text{grid}_A + \text{grid}_B - \text{grid}_{A,B})$ .  
544 Disease-related research effort for each host species was quantified as previously described,  
545 using counts of studies including species names and disease-related terms such as “virus,”  
546 “pathogen”, or “parasite<sup>5</sup>. To fit citation number as a pairwise trait, we took the smaller of a  
547 pair of species' respective citations, and log-transformed the value. Domestication status was  
548 defined *sensu lato*, again as previously described<sup>5</sup>, based on whether a species was ever seen  
549 in a domestic setting. We fit this as a binary pairwise trait where 1=at least one of the species  
550 was domesticated and 0=neither species had been domesticated.

## 551 **Model formulation**

552 We fitted a Generalised Additive Mixed Model (GAMM) to examine which traits influenced  
553 viral sharing among mammal pairs using accelerated discretized implementation in the **mgcv**  
554 package<sup>44</sup>. We fitted viral sharing (0/1) as the response variable, with a binomial family  
555 specification. The model had the following structure:

556

557 Bernoulli(Viral sharing) ~ s(Phylogenetic similarity, by = ordered(Gz)) +  
558 t2(Phylogenetic similarity, Geographic overlap, by = ordered(!Gz)) +  
559 Minimum citation number + Domestication status +  
560 mm (Species 1 + Species 2)

561

562 The first term (“s”) represents a phylogeny effect smooth fitted across species pairs that did  
563 not overlap in space (Gz=1), and “t2” represents a phylogeny:geography tensor product  
564 smooth fitted to species that had geographic overlap greater than zero (Gz=0). This allowed  
565 us to model these two aspects of the data separately, helping us to more effectively model the  
566 large number of spatial zeroes (85% of species pairs did not overlap in space). “mm”  
567 represents a multi-membership random effect, accounting for the identity of both species in  
568 the pair. We implemented this multi-membership effect to control for species-level effects by  
569 including a species-level effect for both the row (Species 1) and column (Species 2) of the  
570 sharing matrix. Using the paraPen specification in **mgcv**, these random effects were  
571 constrained to sample from the same distribution, resulting in a single estimate of the  
572 variance associated with each unique species. Most precisely, these effects in our model help  
573 capture variation in viral sharing that could likely be explained by species-level factors that  
574 are unobserved or otherwise excluded (i.e., differences in underlying viral diversity, which  
575 would be expected to positively impact the probability of interspecific sharing). In sum, this  
576 model formulation allowed us to estimate the effect of pairwise predictors (geographic  
577 overlap, phylogenetic similarity) in determining viral sharing as well as evaluate the  
578 influence of species identity.

579

580 To investigate whether the effects of geography and phylogeny depended on which subset of  
581 viruses we investigated, we fit the model to non-exclusive subnetworks of mammal-mammal  
582 pairs based on the types of viruses they were connected by. Viral subtypes included RNA  
583 viruses (566 hosts sharing 381 viruses); vector-borne RNA viruses (333 hosts sharing 164

584 viruses); non-vector-borne RNA viruses (391 hosts sharing 205 viruses); and DNA viruses  
585 (151 hosts sharing 205 viruses). There were only 2 vector-borne DNA viruses in our data. We  
586 eliminated from each analysis any hosts that were not carrying the focal virus type.

587

588 We elected to use a binary model of viral sharing (0/1) rather than an integer count model  
589 (0+) for two reasons: first, the data distribution was highly skewed, with few very large  
590 values and many zeroes. Under these conditions, we found a count-based model formulation  
591 including species-level random effects computationally intractable. Second, the observed  
592 viral diversity is likely a considerable underestimate, but the extent of this underestimate is a  
593 matter of hot debate<sup>3,4</sup>. As such, the predictions for viral sharing from such a model could be  
594 relative and biased, while binary models offer a more appropriate resolution to quantify  
595 sharing patterns. We wished to avoid estimating a precise number of viruses shared among  
596 pairs of species for this reason.

597

## 598 **Model validation**

599 To check the fit of the model, we predicted 0/1 viral sharing values from the model 1000  
600 times and examined how the values compared to the proportions of 0's and 1's in the  
601 observed data, finding high agreement between the two. We repeated this procedure using a)  
602 the full dataset; b) only the fixed effects, with random effects randomised in each iteration;  
603 and c) only the random effects, with fixed effects held at the mean. We then used these  
604 predicted links to create 1000 unipartite viral sharing networks, estimating link numbers  
605 (degree centrality) for species in each replicated network. We took the mean of these values  
606 across the 1000 replicated networks to give the predicted values displayed in Figure SI1.

607

608 We quantified deviance contributions of our explanatory variables by calculating model  
609 deviance when dropping each variable, and comparing these against the full model and an  
610 intercept-only model deviance. For each of our explanatory variables (geographic overlap,  
611 phylogenetic similarity, minimum citation number, domestication status, and species-level  
612 random effects) we randomised the observed values 1000 times, then predicted sharing  
613 probabilities for these values using our model estimates. This randomisation procedure  
614 allowed us to predict while accounting for the uneven data distribution, rather than using  
615 mean values.

## 616 **Simulating viral sharing networks**

617 Following reconstruction of the observed network as part of our model validation, we  
618 repeated the prediction process on an exhaustive mammal dataset to estimate viral sharing  
619 across all mammals. We set minimum citation number to the data mean, and set  
620 domestication status to 0. We repeated the predictions 1000 times, randomising the species-  
621 level random effects each time. The full prediction dataset included 4196 Eutherian mammals  
622 with known spatial distributions and phylogenetic associations, resulting in 8.8 million  
623 unique pairwise combinations. After predicting 1000 binary sharing networks across all  
624 mammals, we summarised the average predicted link number (degree centrality) of each  
625 species across the 1000 replicates. We then calculated the mean species-level link number  
626 within each mammalian order to examine taxonomic patterns. To project the spatial patterns  
627 of connectedness, we assigned each species range polygon the link number (degree  
628 centrality) of its host species<sup>27</sup> and took the mean value for each grid square, thereby  
629 correcting for species richness. We then repeated these taxonomic and geographic summaries  
630 using within-order and between-order link numbers separately. We also took the summed  
631 values, which more closely reflect underlying patterns of species richness.

632

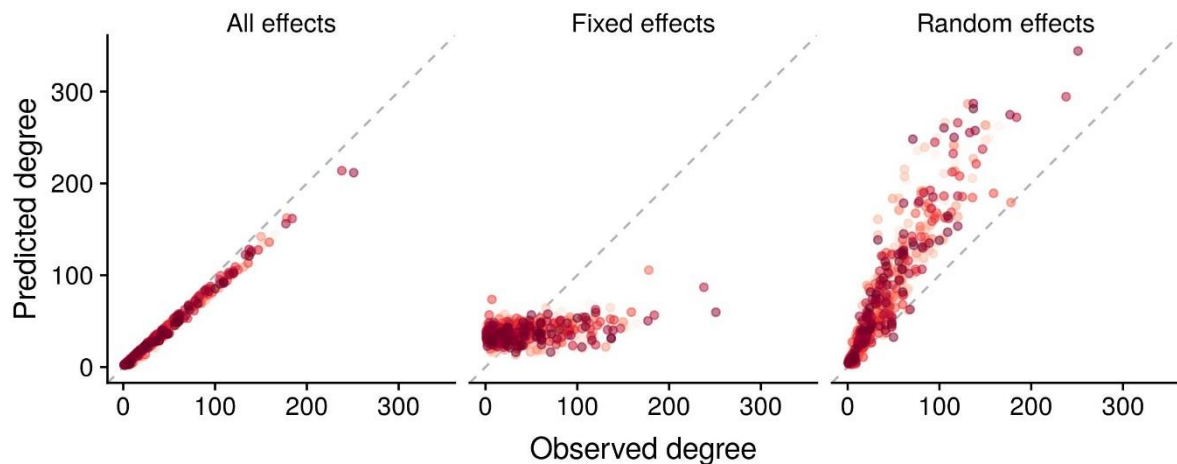
633 We validated the predicted network by comparing it to sharing patterns in the Enhanced  
634 Infectious Diseases Database (EID2)<sup>29</sup>. We eliminated species pairs that were in our training  
635 data and identified whether species pairs that shared viruses in EID2 were more likely to  
636 share viruses in our predicted network than species pairs that did not. In addition, we  
637 investigated whether species that were shown to host zoonoses in our training dataset were  
638 more highly-connected in the predicted network. Finally, we investigated whether species  
639 that were present in only EID2, in only our training data, or in both were more highly-  
640 connected in our predicted network than species that did not appear in either dataset and were  
641 therefore taken to have not been observed hosting a virus.

## 642 **Predicting hosts of focal viruses**

643 To investigate the ability of the model to predict known hosts of viruses in our dataset, we  
644 iteratively investigated the sharing patterns of known hosts independently for all viruses with  
645 >1 host. For each virus, we removed one host at a time, and then investigated which species  
646 the remaining known host species were likely to share viruses with based on the all-mammal  
647 predicted network. If the removed host (“focal host”) was on average highly likely to share

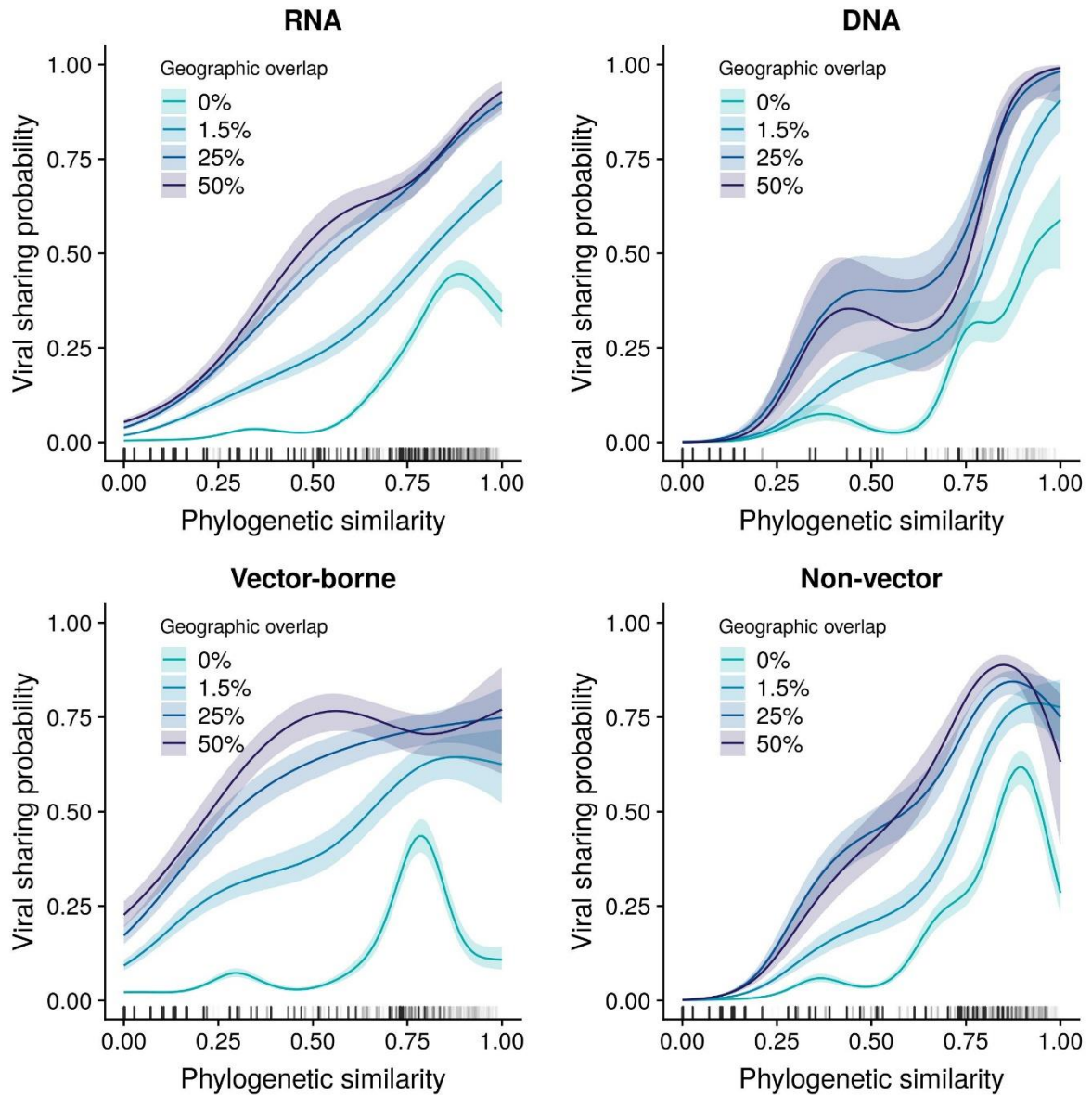
648 viruses with the remaining species, our model was taken to be useful for predicting patterns  
649 of mammal sharing based on known host distributions. The mean ranking of the focal hosts  
650 across each prediction iteration was used as a measure of “predictability” for each virus. We  
651 carried out this process for the 250 viruses with more than one known host with associated  
652 geographic and phylogenetic data and then on the 109 such viruses in the EID2 data.

653 Once the predictability of each virus was calculated, we fitted a linear mixed model  
654 examining  $\log_{10}(\text{mean focal host rank})$  as an inverse measure of predictability (higher rank  
655 corresponds to decreased predictability) for each virus. We added mean phylogenetic host  
656 similarity as a fixed effect and viral family as a random effect to quantify how viral  
657 phylogeny affected predictability. We included additional viral traits in the model, including:  
658 cytoplasmic replication (0/1); segmentation (0/1); vector-borne transmission (0/1); double- or  
659 single-strandedness; DNA or RNA; enveloped or non-enveloped; or zoonotic ability (0/1 for  
660 whether the virus was associated with humans in our dataset).  
661



662

663 Figure S11: Predicted degree centrality of species in our training data network, predicted using our  
664 GAMM estimates. Fixed + random effects were very effective at reproducing individual species’  
665 degree centrality (left); fixed effects were less effective (middle); and random effects alone had a  
666 strong but imperfect effect (right).

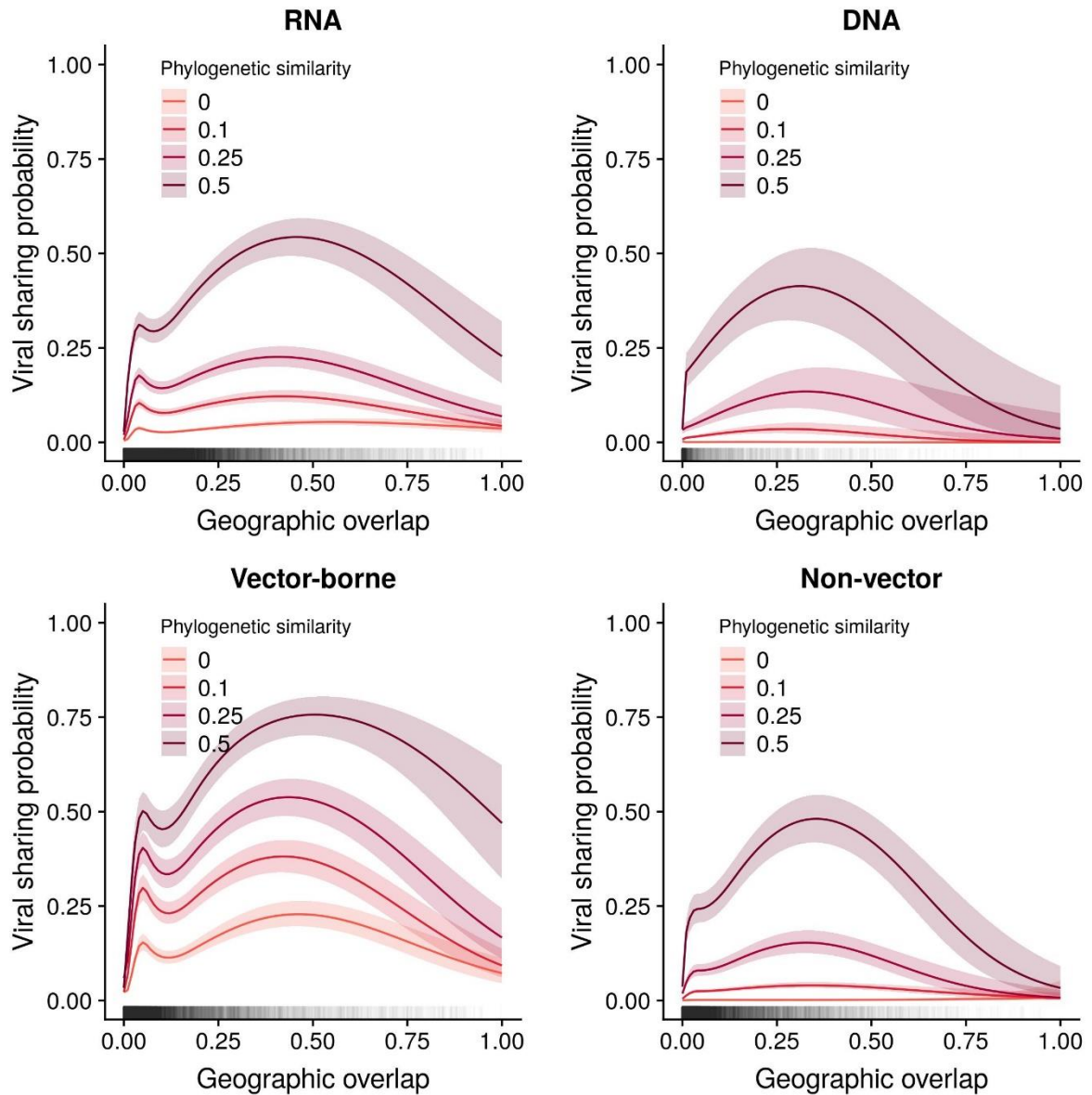


667

668

669 Figure S12: GAMM-derived viral sharing estimates for the effect of phylogenetic similarity for four viral subsets  
670 (top row: all RNA viruses and DNA viruses; bottom row: vector-borne RNA viruses and non-vector-borne RNA  
671 viruses). Each GAMM smooth is displayed at multiple geographic overlap values (different colours).





672

673

674 Figure SI3: GAMM-derived viral sharing estimates for the effect of geographic overlap for four viral subsets  
675 (top row: all RNA viruses and DNA viruses; bottom row: vector-borne RNA viruses and non-vector-borne RNA  
676 viruses). Each GAMM smooth is displayed at multiple geographic overlap values (different colours).

677

678

679

RESPONSE	SAMPLES	DEVIANCE CONTRIBUTIONS					
		Geography	Gz	Phylogeny	Citations	Domestic	Spp
<b>ALL VIRUSES</b>	591	0.077	0.067	0.336	0.005	0.002	0.512
<b>RNA</b>	566	0.079	0.067	0.33	0.005	0.003	0.516
<b>DNA</b>	151	0.008	0.031	0.729	0.001	0.004	0.227
<b>VECTOR-BORNE</b>	333	0.153	0.11	0.145	0	0.008	0.584
<b>NON-VECTOR</b>	391	0.011	0.019	0.625	0.016	0.001	0.328

680

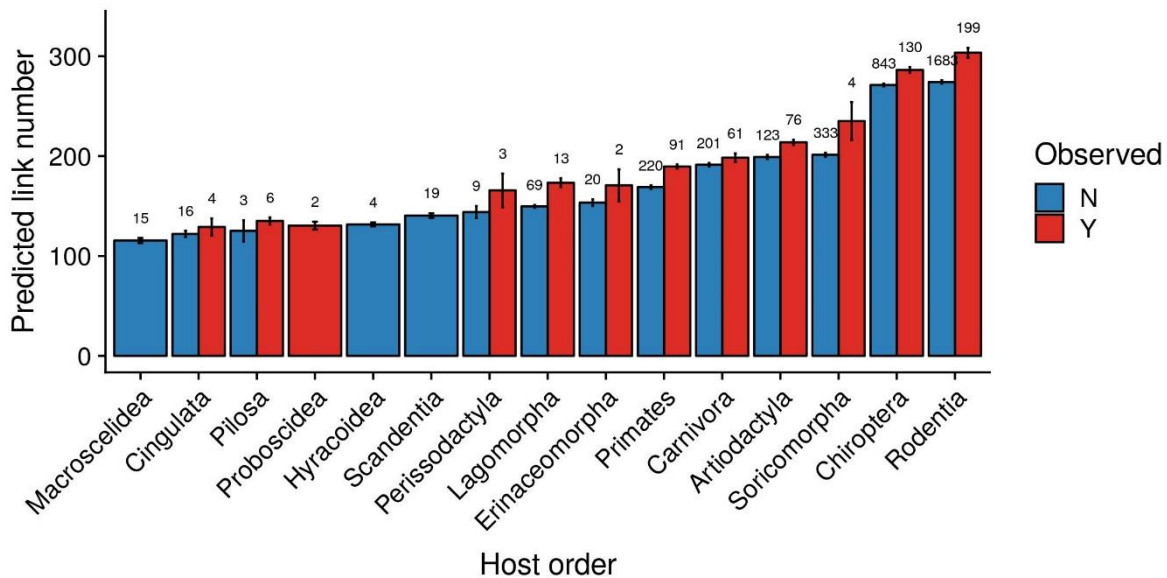
681 Table SI1: The deviance contributions and sample sizes (number of hosts) for each of our viral  
 682 sharing GAMMs. The deviance terms are, in order: proportional geographic overlap; binary  
 683 geographic overlap greater than zero (0/1); phylogenetic similarity; minimum citation number;  
 684 domestication status; and the species-level random effect.

685

686

687

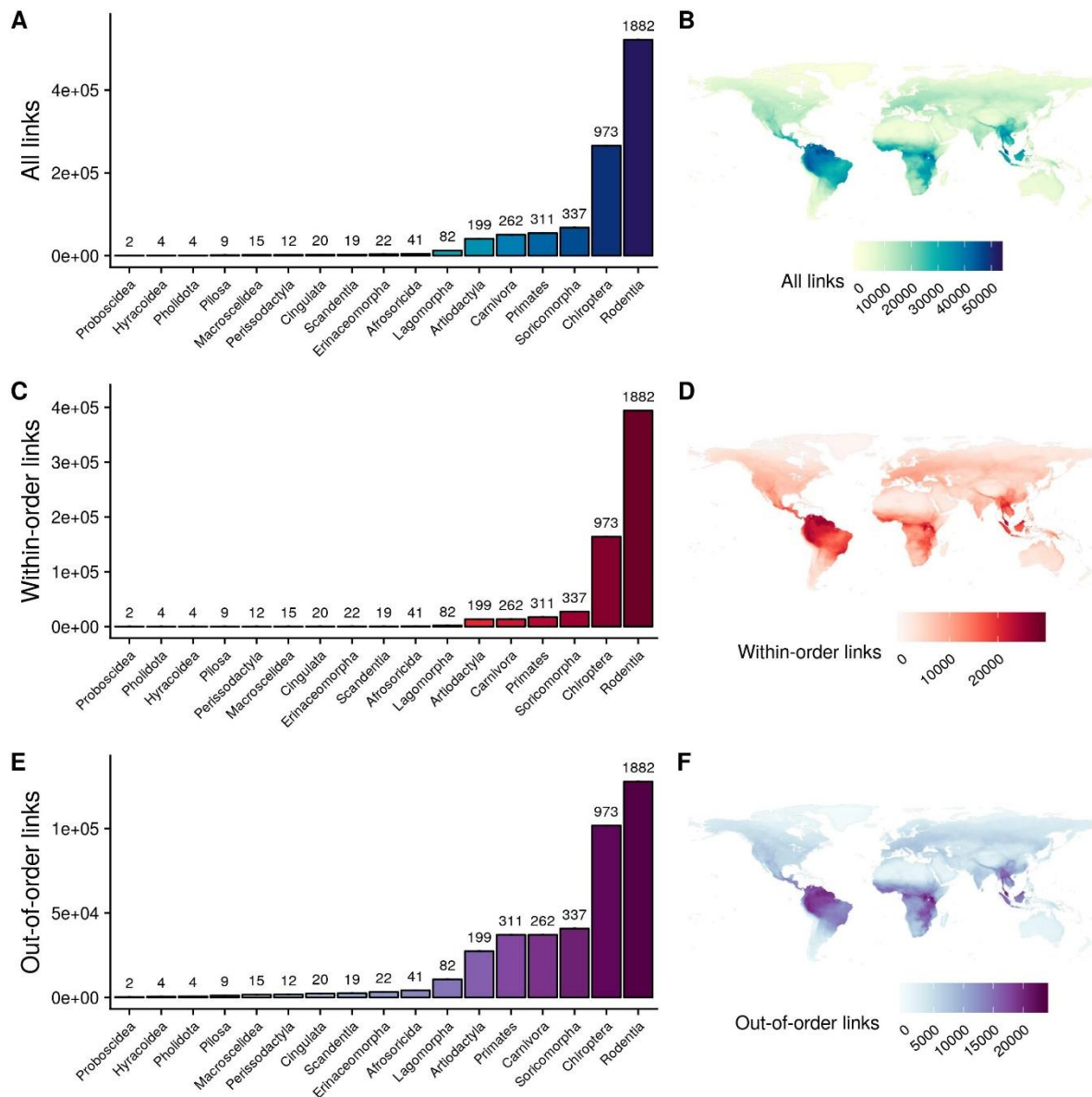
688



689

690 Figure SI4: Mammal species that were observed with at least one virus in the training dataset or the  
 691 EID2 dataset had higher degree centrality (link number) in our predicted network. This figure displays  
 692 the raw data that are displayed in Figure 2C in the main text, but without being scaled within orders.

693



694

695

Figure S15: Taxonomic and geographic patterns of predicted viral link numbers. Top row: all links; middle

696

row: links with species in the same order; bottom row: links with species in another order. A,C,E: summed

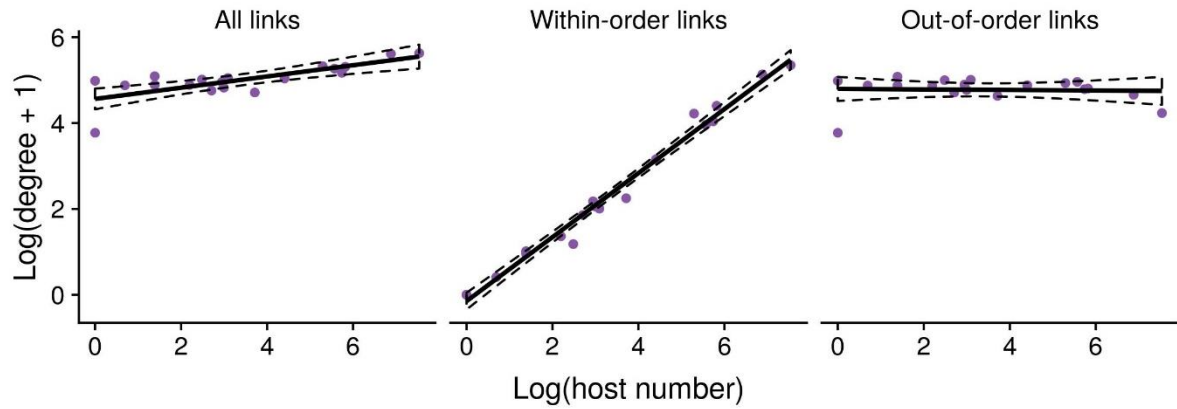
697

species-level link numbers for mammalian orders in our dataset. B,D,F: geographic distributions of link

698

numbers. Distributions were derived by summing the link numbers of all species inhabiting a grid square.

699

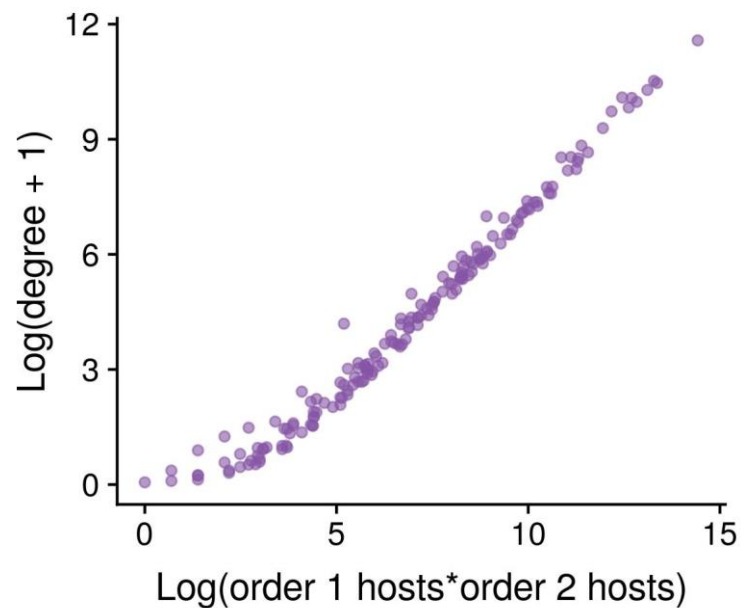


700

701 Figure SI6: Scaling of degree centrality (link numbers) followed a power law when looking within-  
702 orders, but not between orders. The trend line and 95% confidence intervals are derived from a linear  
703 model fitted to the data.

704

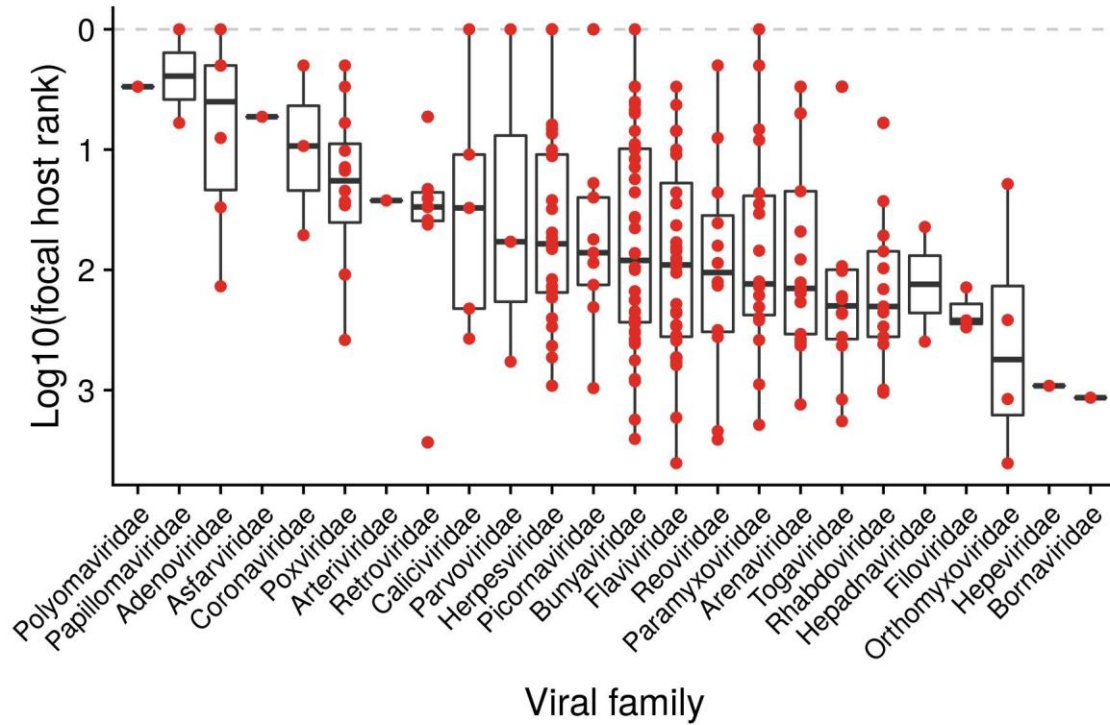
705



706

707 Figure SI7: Predicted between-order link numbers scales according to the log-product of the number  
708 of species in the two orders. Each point represents a pair of orders (N=171).

709

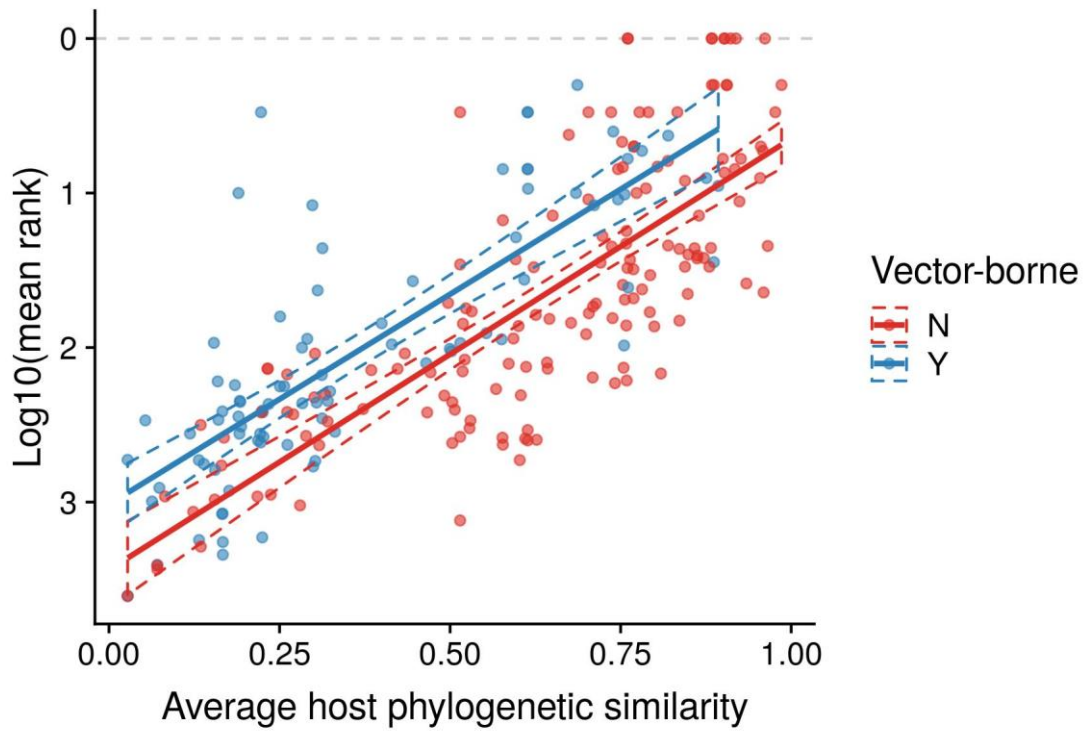


710

711 Figure S18: The phylogeographic predictability of viruses' reservoir hosts varied considerably across  
712 viral families, although the family-level random effect did not account for much of the model's  
713 variance. Families are ordered along the x axis in order of decreasing predictability. The y axis  
714 displays the mean rank of the focal host in our reservoir host prediction simulation, on a reversed  
715 log10-scale. Values closer to the top of the figure represent more predictable viruses.

716

717



718

719 Figure SI9: Viral host range strongly impacted the predictability of reservoir hosts. The x axis  
720 displays the mean phylogenetic similarity of a virus's hosts (i.e., an inverse measurement of viral host  
721 range). The y axis displays the mean rank of the focal host in our reservoir host prediction simulation,  
722 on a reversed log10-scale. Values closer to the top of the figure represent more predictable viruses.

723 The trend lines and 95% confidence intervals were derived from a linear mixed model fitted to the  
724 data.

725